Received September 30, 2018, accepted October 17, 2018, date of publication October 22, 2018,
date of current version November 14, 2018.

Digital Object Identifier 10.1109/ACCESS.2018.2877181

Optimal Distributed Interference Mitigation for Small Cell Networks With Non-Orthogonal Multiple Access: A Locally Cooperative Game

XIANLING WANG[1], (Member, IEEE), HAIJUN ZHANG[2], (Senior Member, IEEE), YUE TIAN[1], (Member, IEEE), CHEN ZHU[1], AND VICTOR C. M. LEUNG[3], (Fellow, IEEE)

[1]Fujian Key Laboratory of Communication Network and Information Processing, Xiamen University of Technology, Xiamen 361024, China
[2]Beijing Advanced Innovation Center for Materials Genome Engineering, Beijing Engineering and Technology Research Center for Convergence Networks and Ubiquitous Services, Institute of Artificial Intelligence, University of Science and Technology Beijing, Beijing 100083, China
[3]Department of Electrical and Computer Engineering, The University of British Columbia, Vancouver, BC V6T 1Z4, Canada

Corresponding author: Haijun Zhang (haijunzhang@ieee.org)

This work was supported in part by the National Natural Science Foundation of China under Grant 61822104, Grant 61471025, Grant 61771044, Grant 61801412, and Grant 61701422, in part by the Natural Science Foundation of Fujian Province, China, under Grant 2016J01323 and Grant 2017J01785, in part by the Young Elite Scientist Sponsorship Program by CAST under Grant 2016QNRC001, in part by the Research Foundation of Ministry of Education of China & China Mobile under Grant MCM20170108, in part by the Beijing Natural Science Foundation under Grant L172025 and Grant L172049, in part by the 111 Project under Grant B170003, and in part by the Fundamental Research Funds for the Central Universities under Grant FRF-GF-17-A6 and Grant RC1631.

ABSTRACT In this paper, we study the potential of non-orthogonal multiple access (NOMA) for the purpose of interference mitigation in downlink small cell networks (SCNs). Different from prior works, we focus on opportunistically multiplexing different users on the same subchannel to avoid the severe inter-cell interference brought in by ultradense networking. Aiming to maximize the network throughput, we formulate a distributed subchannel assignment problem with local information exchange. This problem is analyzed through a locally cooperative game model, and the existence of Nash equilibrium (NE) is confirmed by proving that the formulated game is an exact potential game. To solve the problem, we design two concurrent distributed algorithms based on best response (BR) and spatial adaptive play (SAP), respectively. The BR-based algorithm guarantees rapid convergence to an NE, which may not be globally optimal. On the contrary, the SAP-based algorithm can find the global optimum with an arbitrary large probability, although the learning process requires more iterations to converge. Simulation results reveal that the aggregate interference can be more efficiently suppressed in NOMA enhanced networks, which can lead to higher network throughputs. Besides, the superiority of NOMA over orthogonal multiple access is more obvious when the network grows denser.

INDEX TERMS Distributed algorithm, global optimality, interference mitigation, locally cooperative game, Nash equilibrium, non-orthogonal multiple access, potential game.

I. INTRODUCTION

Due to the rapid proliferation of smart devices, the fifth generation (5G) wireless networks are expected to face an unprecedented growth in the amount of subscribers and data traffics. For instance, by the end of 2020, the number of connected devices will reach 50 billion with diverse service requirements, while the traffic data volume is predicted to be 1000 times larger than that in 2010 [1]. In this context, small cell network (SCN) has been emerging as a promising network architecture to meet the overwhelming traffic demand [2], [3]. By densely deploying low-power small cell base stations (SBSs), the SCN can provide a multitude of benifits, including expanded indoor and blind spot coverage, enhanced spectrum spatial reuse, and reduced power consumption.

Besides SCN, advanced physical layer techniques have also drawn much attentions recently, and these techniques include millimeter wave (mmWave) communications [4], massive multiple-input multiple-output (MIMO) [5], and non-orthogonal multiple access (NOMA) [6]. Among them, NOMA is foreseen as a potential alternative due to its capability of providing massive connectivity and achieving higher spectrum efficiency within limited bandwidth resources [7]. The superiority of NOMA over conventional orthogonal multiple access (OMA), such as orthogonal frequency division multiple access (OFDMA) in long term evolution (LTE), lies in the fact that NOMA smartly reuse the same resource block to serve multiple users simultaneously. This is realized by utilizing the superposition coding technology and multiplexing the signals of different users in the power domain with different power levels at the transmitter side. With successive interference cancellation (SIC) equipped at the receiver side, the superimposed signals of different users can be separated correctly. Therefore, implementing SCN with NOMA is regarded as one of the most promising solutions to meet the challenges in 5G wireless networks and beyond [8].

A. RELATED WORKS AND MOTIVATION

Since the initial research in [9] introduced NOMA to improve cell-edge user throughput performance, several topics in this context were discussed. Some researchers have focused on investigating the performance improvement brought in by integrating NOMA with other technologies [10]–[14]. Ding *et al.* [10] designed a NOMA enhanced MIMO scheme to support short packet transmissions in internet of things (IoT). The proposed scheme can solve the problem when users are sharing similar channel states, which impairs the implementation of NOMA. Jia *et al.* [15] extended NOMA to a dual non-orthogonal version to address the spectrum efficiency and security issues in IoT. In [16], the interplay between NOMA and coordinated multi-point transmission (CoMP) was studied, and an opportunistic NOMA selection strategy was design to improve the system performance. Thanks to the well developed mathematical tools provided by stochastic geometry, the performance gain of NOMA was also evaluated under large-scale network models. In [12] and [13], the system performance of NOMA in multimedia broadcast/multicast service transmissions and user centric networks were studied, respectively, under the basic Poisson point process (PPP) model. Tabassum *et al.* [14] applied Poisson cluster process model to study the system performance of NOMA enhanced uplink cellular networks, and the influence of imperfect SIC was also taken into consideration.

In addition, various resource allocation problems for NOMA enhanced networks were also addressed in the literature. In this field, the newly developed matching game model provides efficient tools to solve the user pairing problem introduced by NOMA. Based on matching game model, subchannel assignment and user scheduling problem to maximize the sum rate while considering users' fairness were addressed for downlink single-cell NOMA networks in [17] and for NOMA enhanced heterogeneous networks in [18]. The work in [19] proposed a low complexity algorithm to determine the subchannel assignment and power proportional factors between NOMA users to realize optimization from the energy efficiency perspective. Taking one step further, the balance between energy efficiency and delay of NOMA enhanced network was considered in [20]. Also taking energy efficiency into consideration, the work in [21] addressed the joint base station association and power control optimization problem. Aiming to maximize the long-term network utility, the data rate control and the power allocation were jointly optimized by leveraging the Lyapunov optimization framework in [22].

In the meantime, under the network densification trend and the realization of massive connection scenarios such as IoT, interference mitigation still remains a hot topic in recent years [23]–[25]. For such ultra dense network scenarios, an enormous increase in information exchange overhead is expected for traditional centralized optimization approaches, and this promotes the trend of solving interference mitigation problems through distributed approaches. To this end, the interaction between independent SBSs is usually analyzed under the game theory framework, which provides powerful tools to study the equilibrium of the networks [26]. In [27], a local cooperation game was formulated to analyze the joint power allocation and user scheduling problem, and efficient distributed interference mitigation algorithms were proposed. Xu *et al.* [28] considered multi-user SCN interference mitigation problems, in which a distributed spectrum access algorithm was proposed based on graphical games. The work in [29] and [30] both applied user demand related metrics as the network utility, and distributed interference avoidance solutions were devised by exploiting a local interaction game.

Although several recent works have addressed subchannel assignment problems in NOMA based networks and distributed interference mitigation, few effort has been put in exploring the potential of NOMA to mitigate inter-cell interference in the SCN. In traditional interference mitigation problems, it is desirable to reduce the number of neighboring SBSs choosing the same subchannels [28]–[30]. Naturally, the principle of NOMA is in line with this basic idea. For example, by opportunistically applying NOMA and multiplexing different users on one subchannel, a SBS can release its occupancy of other subchannels and thus eliminate its interference to nearby SBSs. Therefore, it is attractive to investigate how to coordinate NOMA and subchannel assignment for the purpose of interference mitigation and devise efficient strategies to fully exploit the potential of NOMA, especially in a distributed manner. A preliminary investigation on this problem was published in [31], and this work mainly extends [31] in the following ways: 1) The throughput based utility is considered instead of the aggregate interference. 2) A new distributed learning algorithm is proposed in this paper, which provides better converged throughput performance.

B. CONTRIBUTIONS

In this paper, we investigate the distributed subchannel assignment problem for the purpose of interference mitigation in the SCN, where NOMA is enabled in the SBS to multiplex different users on the same subchannel. We aim to maximize the sum throughput of all users over the network.

To this end, we formulate a locally cooperative game, in which information is locally exchanged among neighboring SBSs. Based on distributed learning technology, we propose two efficient algorithms and achieve desirable solutions for the problem. The main contributions of this paper are summarized as follows.

- We introduce local cooperation between neighboring SBSs to fully exploit the potential of NOMA, which relies on its altruistic feature in interference mitigation. Specifically, we formulate a locally cooperative game, in which each SBS considers the throughput of itself as well as its neighboring SBSs rather than the throughput of itself only. The formulated game is proved to be an exact potential game with the network throughput being the potential function. Therefore, at least one Nash equilibrium (NE) exists in the game, corresponding to the globally or locally optimal solution to the distributed subchannel assignment problem.
- We design two concurrent distributed algorithms, i.e., the concurrent best response (C-BR) algorithm and the concurrent spatial adaptive play (C-SAP) algorithm, to achieve the NE of the game. The designed concurrent algorithms allow several SBSs to act simultaneously and are more efficient than their traditional versions, in which only one SBS can change its strategy at a time. The convergence property of the two algorithms are analytically proved. It is shown in the simulation results that the C-BR iteration rapidly converge to an NE of the game, but this rapid converging speed is at the cost of the efficiency of global optimality. On the contrary, the C-SAP algorithm can find the global optimum with an arbitrary large probability, although the learning process requires more iterations to converge.
- We show that by opportunistically applying NOMA in the SCN, the inter-cell interference caused by neighboring SBSs can be more efficiently mitigated. This will bring in higher network throughput for the NOMA enhanced SCNs than that for traditional OMA based networks, in which a subchannel can be allocated to no more than one user in a SBS. Simulation results also show that NOMA is more attractive when the density of the network increases, confirming the superiority of NOMA over traditional OMA under the trend of ultra dense networking.

The rest of the paper is organized as follows. Detailed descriptions of system model and problem formulation are given in Section II. A locally cooperative game model and two proposed distributed learning algorithms are presented in Section III and IV, respectively. Simulation results and observations are discussed in Section V. Finally, conclusions are drawn in Section VI.

II. SYSTEM MODEL AND PROBLEM FORMULATION

A. SYSTEM MODEL

We consider a downlink SCN consisting of N SBSs operating on the same spectrum. The SBS set is denoted by $\mathcal{N} = \{\mathrm{SBS}_1, \cdots, \mathrm{SBS}_n, \cdots, \mathrm{SBS}_N\}$, where SBS_n is the n-th SBS in $\mathcal{N}$. The spectrum is equally divided into M subchannels, and the subchannel set is denoted by $\mathcal{M} = \{\mathrm{CH}_1, \cdots, \mathrm{CH}_m, \cdots, \mathrm{CH}_M\}$, where CH_m is the m-th subchannel in $\mathcal{M}$. The set of user equipments (UEs) associated with SBS_n is denoted by $\mathcal{K}_n = \{\mathrm{UE}_{n,1}, \cdots, \mathrm{UE}_{n,k}, \cdots, \mathrm{UE}_{n,K_n}\}$, where $\mathrm{UE}_{n,k}$ is the k-th UE of SBS_n and K_n is the number of UEs served by SBS_n. Assume that SIC receiver is enabled at each UE, so that the SBSs can choose NOMA to serve its associated UEs. Compared with OMA, NOMA reduces the number of subchannels for a SBS when multiple UEs are associated to it. Take $K_n = 2$ as an example, in which SBS_n needs two subchannels to serve its associated UEs in OMA networks. But with NOMA capability, SBS_n can multiplex these two UEs on one subchannel. An example of the considered system model is shown in Fig. 1. Also assume that no central controller is setup in the network. Hence each SBS assigns subchannels in a distributed manner.

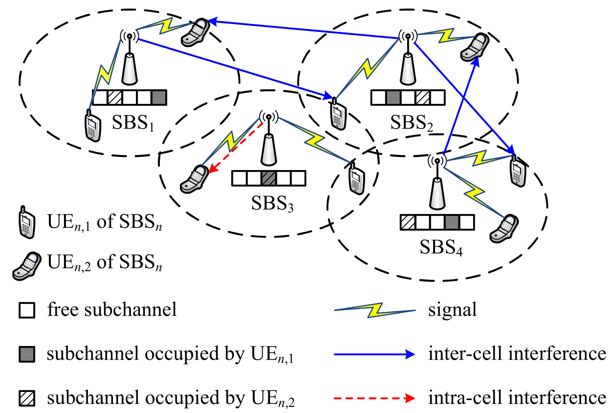

FIGURE 1. An example of SCN with NOMA, where each SBS is associated with two UEs: 1) SBS_1, SBS_2 and SBS_4 apply OMA so each of them occupies two subchannels to serve their associated UEs, while SBS_3 applies NOMA and occupies only one subchannel. 2) Inter-cell interference exists between SBS_1 and SBS_2, as well as SBS_2 and SBS_4 due to common subchannel occupancy, and the inter-cell interference is asymmetric. 3) $\mathrm{UE}_{3,2}$ experiences intra-cell interference instead of inter-cell interference because no other SBSs is transmitting on the same subchannel.

B. INTER-CELL INTERFERENCE

Assume that SBS_n transmits with fixed power p_n on each subchannel. The received signal power at $\mathrm{UE}_{i,k}$ from SBS_n is modeled as $p_n d_{n,i,k}^{-\alpha}$, where $d_{n,i,k}^{-\alpha}$ is the channel power gain based on distance $d_{n,i,k}$ from SBS_n to $\mathrm{UE}_{i,k}$, and $\alpha > 2$ is the path-loss exponent. This propagation model is widely used as in [14], [29], and [32]. The interference effect between two SBSs is characterized by the interference metric (IM) [27], which is defined as

$$I_{\mathrm{m}}(n,i) = \frac{1}{K_i}\sum_{k=1}^{K_i}\frac{p_n d_{n,i,k}^{-\alpha}}{p_i d_{i,i,k}^{-\alpha}}, \tag{1}$$

where $d_{i,i,k}$ is the transmission link distance for $\mathrm{UE}_{i,k}$. $I_{\mathrm{m}}(n,i)$ denotes the interference level from SBS_n to SBS_i, and is normalized to the desired signal power. Obviously, the interference relationship between SBS_i and SBS_n is asymmetric, i.e., $I_m(n, i) \neq I_m(i, n)$.

Since the SBSs are spatially scattered and the signal power is severely attenuated after long-distance transmission, a SBS will only interfere UEs of its neighboring SBSs. Hence, to build up the potential interference relationship between SBSs, we resort to the interference graph $G_{IM} = \{\mathcal{N}, \mathcal{E}\}$ [27], [28], [33], where the SBS set $\mathcal{N}$ constitutes the vertex set, and $\mathcal{E}$ is the edge set. G_{IM} is constructed based on IM. Specifically, a directional edge (n, i) is setup from SBS_n to SBS_i if $I_m(n, i)$ is greater than a predefined interference threshold I_{th}, implying that SBS_n is causing nonnegligible interference effect to SBS_i. So we have $\mathcal{E} = \{(n, i)|SBS_n \in \mathcal{N}, SBS_i \in \mathcal{N}, I_m(n, i) \geq I_{th}\}$. Based on $\mathcal{E}$, we define $\mathcal{J}_n = \{SBS_i|SBS_i \in \mathcal{N}, (i, n) \in \mathcal{E}\}$ accounting for the set of SBSs causing nonnegligible interference to SBS_n, and $\mathcal{Z}_n = \{SBS_i|SBS_i \in \mathcal{N}, (n, i) \in \mathcal{E}\}$ accounting for the set of SBSs being disturbed by SBS_n. $\mathcal{J}_n$ and $\mathcal{Z}_n$ determine the potential interference relationship between SBS_n and its nearby SBSs. However, inter-cell interference will not occur on an occupied subchannel for SBS_n unless two or more SBSs in $\mathcal{J}_n$ are transmitting on this subchannel as well. An example of G_{IM} is shown in Fig. 2.

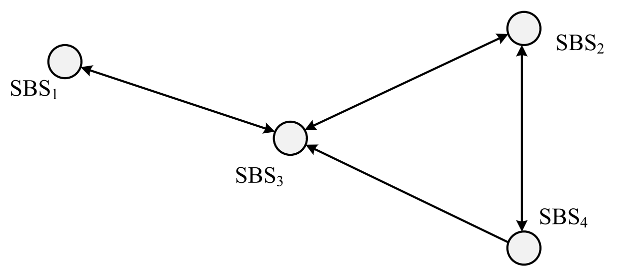

FIGURE 2. An example of G_{IM} corresponding to the network topology given in Fig. 1: 1) No edge exists between SBS_1 and SBS_2, because SBS_1 lies at a distance away from SBS_2 and the mutual interference between these two SBSs can be neglected. 2) Directional edge exists from SBS_4 to SBS_3, revealing the asymmetric interference relationship between these two SBSs. This also leads to the difference between $\mathcal{Z}_3$ and $\mathcal{J}_3$, where $\mathcal{Z}_3 = \{SBS_1, SBS_2\}$ and $\mathcal{J}_3 = \{SBS_1, SBS_2, SBS_4\}$. 3) G_{IM} only represents the potential interference relationship between SBSs. Although edges exist between SBS_2 and SBS_3, these two SBSs are not sharing any common subchannel so the received signals in these two SBSs are not affected by each other.

Assume that SBS_n allocates only one subchannel to a UE. Denote by $\mathbf{a}_n = \{CH_{n,1}, \cdots, CH_{n,k}, \cdots, CH_{n,K_n}\}$ the vector of designated subchannels of SBS_n, where $CH_{n,k}$ is the selected subchannel for $UE_{n,k}$. So the aggregate inter-cell interference $I_{\text{inter}}^{(n,k)}$ of $UE_{n,k}$ is calculated by

$$I_{\text{inter}}^{(n,k)} = \sum_{i=1}^{|\mathcal{J}_n|} p_i d_{i,n,k}^{-\alpha} \delta(i, n, k), \tag{2}$$

where $|\cdot|$ is the cardinality of the set, and $\delta(i, n, k)$ is an indicator function given by

$$\delta(i, n, k) = \begin{cases} 1, & CH_{n,k} \in \mathbf{a}_i, \\ 0, & CH_{n,k} \notin \mathbf{a}_i. \end{cases} \tag{3}$$

Note that, in $\mathbf{a}_n$, repeating elements may exist for the NOMA system, while each element is unique for the NOMA system. Let $\mathcal{A}_n$ be the available action set of SBS_n. Therefore, we have $|\mathcal{A}_n| = M^{K_n}$ for the NOMA system, and $|\mathcal{A}_n| = M(M-1)\cdots(M-K_n+1)$ for the OMA system.

C. INTRA-CELL INTERFERENCE

When a SBS apply NOMA to transmit signals for two UEs in the downlink systems, the superimposed signal will lead to intra-cell interference among these two UEs. In order to eliminate the intra-cell interference, each UE is assumed to be equipped with SIC. To achieve high efficiency, a SIC usually decodes the signal with higher power and then cancells it before the detection of the signal with lower power. To characterize the intra-cell interference introduced by NOMA, we define $\widehat{\mathcal{K}}_{n,k}$ and $\widetilde{\mathcal{K}}_{n,k}$ representing the sets of UEs, which are with higher channel gain and lower channel gain than $UE_{n,k}$, respectively, and are also being served by SBS_n on $CH_{n,k}$. So we have

$$\widehat{\mathcal{K}}_{n,k} = \left\{UE_{n,j}|d_{n,n,k}^{-\alpha} < d_{n,n,j}^{-\alpha}, CH_{n,j} = CH_{n,k}\right\}, \tag{4}$$

$$\widetilde{\mathcal{K}}_{n,k} = \left\{UE_{n,j}|d_{n,n,k}^{-\alpha} > d_{n,n,j}^{-\alpha}, CH_{n,j} = CH_{n,k}\right\}, \tag{5}$$

$$\begin{aligned} \mathcal{K}_{n,k} &= \left\{UE_{n,j}|CH_{n,j} = CH_{n,k}\right\} \\ &= \widehat{\mathcal{K}}_{n,k} \cup \widetilde{\mathcal{K}}_{n,k} \cup \left\{UE_{n,k}\right\}, \end{aligned} \tag{6}$$

where $\mathcal{K}_{n,k}$ represents the set of UEs which are served on the same subchannel $CH_{n,k}$ including $UE_{n,k}$ itself. Note that if $CH_{n,k}$ is only designated to $UE_{n,k}$ in SBS_n, we will have $\widehat{\mathcal{K}}_{n,k} \cup \widetilde{\mathcal{K}}_{n,k} = \emptyset$, $\mathcal{K}_{n,k} = \left\{UE_{n,k}\right\}$, and $\left|\mathcal{K}_{n,k}\right| = 1$. In addition, to improve fairness, a SBS should allocate more transmit power to the UE with weaker channel gain to improve its received signal quality [7]. Assume that transmit power p_n on $CH_{n,k}$ is divided to the UEs according to their channel gain as in [9] given by

$$p_{n,k} = p_n \cdot \frac{\left(d_{n,n,k}^{-\alpha}\right)^{-\eta}}{\sum_{UE_{n,j} \in \mathcal{K}_{n,k}} \left(d_{n,n,j}^{-\alpha}\right)^{-\eta}}, \tag{7}$$

where η $(0 \leq \eta \leq 1)$ is a decay factor to adjust user fairness. It is revealed in (7) that the signals designated to UEs with weaker channel gain are transmitted with more power. So according to the principle of optimal decoding order, at $UE_{n,k}$, we have that: 1) The received signals for UEs within $\widetilde{\mathcal{K}}_{n,k}$ is with higher power and can be cancelled through SIC, i.e., $UE_{n,k}$ will not suffer intra-cell interference from signals that are designated for UEs in $\widetilde{\mathcal{K}}_{n,k}$. 2) The received signals for UEs within $\widehat{\mathcal{K}}_{n,k}$ is with lower power and cannot be cancelled, i.e., $UE_{n,k}$ will suffer intra-cell interference from signals that are designated for UEs in $\widehat{\mathcal{K}}_{n,k}$. 3) No intra-cell interference will occur if $\left|\mathcal{K}_{n,k}\right| = 1$, i.e., $UE_{n,k}$ will not suffer intra-cell interference if $CH_{n,k}$ is only designated to it in SBS_n.

In consequence, the intra-cell interference $I_{\text{intra}}^{(n,k)}$ experienced by $\text{UE}_{n,k}$ is calculated by

$$I_{\text{intra}}^{(n,k)} = \sum_{\text{UE}_{n,j} \in \widehat{\mathcal{K}}_{n,k}} p_{n,j} d_{n,n,k}^{-\alpha}. \tag{8}$$

Multiplexing different UEs on the same subchannel through NOMA introduces intra-cell interference. However, if NOMA is applied in an opportunistic manner, the intra-cell and inter-cell interference can be balanced. In specific, the expected benefits are as follows: 1) When a SBS senses a limited number of subchannels that are experiencing low inter-cell interference [34], this SBS can apply NOMA to multiplex different UEs on these subchannels to avoid the high inter-cell interference on other subchannels. This advantage motivates SBSs to apply NOMA because it meets with the selfish nature of an individual SBS. 2) A SBS can proactively apply NOMA and release its occupancy of some other subchannels. This altruistically reduces the chance of interfering its neighboring SBSs and may be beneficial for the whole network, although the benefit of this SBS may be impaired. In this case, incenting SBSs to apply NOMA by individual benefit may be inefficient, for which, we will introduce local cooperation between neighboring SBSs in the following.

D. PROBLEM FORMULATION

Define the subchannel assignment strategy profile for all SBSs as $\mathbf{A} = \{\mathbf{a}_1, \cdots, \mathbf{a}_n, \cdots, \mathbf{a}_N\}$. Given the strategy profile $\mathbf{A}$, the throughput of $\text{UE}_{n,k}$ is calculated

$$C_{n,k}(\mathbf{A}) = B \log_2 \left(1 + \frac{p_{n,k} d_{n,n,k}^{-\alpha}}{I_{\text{inter}}^{(n,k)} + I_{\text{intra}}^{(n,k)} + \sigma^2}\right), \tag{9}$$

where B is the bandwidth of a subchannel, and σ^2 is the power of the additive white Gaussian noise. We focus on the sum throughput as the key metric instead of the aggregate interference in this paper. This is because the throughput is more concerned than the experienced interference from the perspective of both the network operators and the users. Meanwhile, in the context of interference mitigation, a higher throughput usually results from a lower aggregate interference level. Thus, we set the network utility as the sum throughput of all UEs in the network, which is expressed as

$$U(\mathbf{A}) = \sum_{n=1}^{N} \underbrace{\sum_{k=1}^{K_n} C_{n,k}(\mathbf{A})}_{C_n(\mathbf{A})}. \tag{10}$$

We aim to maximize the sum throughput of the network, so the interference mitigation problem of multiple UE subchannel assignment in SCN with NOMA is formulated as

$$\text{P1}: \qquad \mathbf{A}_{\text{opt}} = \arg\max U(\mathbf{A}), \tag{11}$$

which can be interpreted as finding the optimal subchannel assignment strategy to maximize the sum throughput of all UEs in the network. It should be noted that when different type of BSs coexist in the network, the network utility in (10) can be changed into a weighted form to balance the interference mitigation performance between the macro cell base stations (MBSs) and the SBSs. For example, to guarantee higher priority for the UEs of the MBSs, a larger weight can be assigned to this UEs.

III. LOCALLY COOPERATIVE GAME

In this paper, we assume that there is no central controller in the system. This assumption is very common in SCN, because coordinating densely deployed SBSs through a central controller requires a large amount of overhead for information exchange. Besides, P1 is evidently a combinatorial optimization problem and solving such problem through centralized approaches is NP-hard. Therefore, we focus on self-organized and distributed approaches with low information exchange requirement. We will firstly resort to game theoretic model to study the interaction between SBSs.

A. LOCALLY COOPERATIVE GAME MODEL

Due to the low complexity, we apply non-cooperative game model to capture the self-determining nature of SBSs. In this game model, each SBS is assumed to be always choosing a strategy that can maximize its own utility. But as previously mentioned, acting in a totally selfish manner cannot fully exploit the potential of NOMA to mitigate interference, and is inefficient from the perspective of the whole network. To overcome this deficiency while maintaining a low complexity, we introduce local cooperation between neighboring SBSs under the framework of non-cooperative game model. This is achieved by designing for each SBS a utility function that integrates the interests of itself and its neighboring SBSs. The modified non-cooperative game, which we term locally cooperative game, is denoted by

$$\mathcal{G} = \left\{\mathcal{N}, G_{\text{IM}}, \{\mathcal{A}_n\}_{\text{SBS}_n \in \mathcal{N}}, \{u_n\}_{\text{SBS}_n \in \mathcal{N}}\right\}, \tag{12}$$

where $\mathcal{N} = \{\text{SBS}_1, \cdots, \text{SBS}_N\}$ is the set of players, G_{IM} is the interference graph describing the neighboring relationship between SBSs, $\mathcal{A}_n$ is the available action set of SBS_n, and u_n is the utility function of SBS_n.

To motivate locally altruistic action for SBS_n, the throughput of SBSs in $\mathcal{Z}_n$ are taken into consideration in utility function u_n of SBS_n as

$$\begin{aligned} &u_n(\mathbf{a}_n, \mathbf{a}_{-n}) \\ &= C_n(\mathbf{a}_n, \mathbf{a}_{-n}) + \sum_{\text{SBS}_j \in \mathcal{Z}_n} C_j(\mathbf{a}_n, \mathbf{a}_{-n}) \\ &= \sum_{k=1}^{K_n} B \log_2 \left(1 + \frac{p_{n,k} d_{n,n,k}^{-\alpha}}{I_{\text{inter}}^{(n,k)} + I_{\text{intra}}^{(n,k)} + \sigma^2}\right) \\ &\quad + \sum_{\text{SBS}_j \in \mathcal{Z}_n} \sum_{k=1}^{K_j} B \log_2 \left(1 + \frac{p_{j,k} d_{j,j,k}^{-\alpha}}{I_{\text{inter}}^{(j,k)} + I_{\text{intra}}^{(j,k)} + \sigma^2}\right), \end{aligned} \tag{13}$$

where $\mathbf{a}_n \in \mathcal{A}_n$ is the action of SBS_n, and $\mathbf{a}_{-n}$ is the action profile of all SBSs except SBS_n.

From (13), we can see that the utility of SBS_n includes two parts: 1) The throughput of all UEs associated with SBS_n; 2) The throughput of all UEs associated with all SBSs which are interfered by SBS_n, i.e., $\mathrm{SBS}_j \in \mathcal{Z}_n$. Therefore, information exchange is necessary among SBS_n and its neighboring SBSs to obtain the utility. In specific, SBSs in $\mathcal{J}_n \cup \mathcal{Z}_n$ should report their current strategies, while SBSs in $\mathcal{Z}_n$ should also report the signal powers and the aggregate interference powers their associated UEs suffered. The amount of information exchange is determined by the size of $\mathcal{J}_n$ and $\mathcal{Z}_n$, and hence by the interference threshold I_{th}. Note that a larger I_{th} reduces the amount of information exchange but will impair the accuracy of the reported interference information. A smaller I_{th} increases the accuracy but a SBS will need to exchange information with more SBSs. When $I_{\text{th}} = 0$, a SBS will need to exchange information with all other $N-1$ SBSs in the network.

Finally, the locally cooperative game can be equivalently expressed as

$$\mathcal{G}: \max_{\mathbf{a}_n \in \mathcal{A}_n} u_n\left(\mathbf{a}_n, \mathbf{a}_{-n}\right), \quad \forall \mathrm{SBS}_n \in \mathcal{N}. \tag{14}$$

B. ANALYSIS OF NASH EQUILIBRIUM

In the formulated locally cooperative game, the strategy space for each SBS is greatly enlarged by NOMA. Hence it is important to investigate if this game holds any steady state as conventional OMA systems [28], [33]. To this end, we resort to the Nash equilibrium (NE), which is formally definined in Definition 1.

Definition 1 (Nash Equilibrium): A subchannel assignment strategy profile $\mathbf{A}^* = \left\{\mathbf{a}_1^*, \cdots \mathbf{a}_n^*, \cdots \mathbf{a}_N^*\right\}$ is a pure strategy Nash equilibrium if no unilateral deviation in strategy by any single player can improve the utility for that player, that is

$$u_n\left(\mathbf{a}_n^*, \mathbf{a}_{-n}^*\right) \geq u_n\left(\mathbf{a}_n, \mathbf{a}_{-n}^*\right), \quad \forall \mathrm{SBS}_n \in \mathcal{N}, \quad \forall \mathbf{a}_n \in \mathcal{A}_n, \mathbf{a}_n \neq \mathbf{a}_n^*. \tag{15}$$

Any NE is a steady state in the game because no player has incentive to change its current strategy. Next, we prove the existence of NE in the formulated game in Theorem 1.

Theorem 1: The formulated game $\mathcal{G}$ is an exact potential game which has at least one pure strategy NE. Moreover, the solution $\mathbf{A}_{\text{opt}}$ for problem P1 is also a NE of $\mathcal{G}$.

Proof: We start by constructing a potential function as

$$\begin{aligned}\Phi\left(\mathbf{a}_n, \mathbf{a}_{-n}\right) &= \sum_{l=1}^{N} C_l\left(\mathbf{a}_n, \mathbf{a}_{-n}\right) = \sum_{l=1}^{N}\sum_{k=1}^{K_l} B\log_2 \\ &\times\left(1+\frac{p_{l,k}d_{l,l,k}^{-\alpha}}{I_{\text{inter}}^{(l,k)}\left(\mathbf{a}_n, \mathbf{a}_{-n}\right)+I_{\text{intra}}^{(l,k)}\left(\mathbf{a}_n, \mathbf{a}_{-n}\right)+\sigma^2}\right),\end{aligned} \tag{16}$$

where $I_{\text{inter}}^{(l,k)}\left(\mathbf{a}_n, \mathbf{a}_{-n}\right)$ and $I_{\text{intra}}^{(l,k)}\left(\mathbf{a}_n, \mathbf{a}_{-n}\right)$ are the aggregate inter-cell and intra-cell interference of the k-th UE of SBS_l when SBS_n choose action $\mathbf{a}_n$ and other SBSs choose action profile $\mathbf{a}_{-n}$. This definition is identical with the network utility defined in (10). According to G_{IM}, the SBS set $\mathcal{N}$ can be divided into 3 disjoint subsets, i.e., $\{\mathrm{SBS}_n\}$, $\mathcal{Z}_n$, and $\mathcal{T}_n = \mathcal{N} \backslash \left(\mathcal{Z}_n \cup \mathrm{SBS}_n\right)$, where $\mathcal{A}\backslash\mathcal{B}$ represents excluding the elements of $\mathcal{B}$ from $\mathcal{A}$. So $\Phi\left(\mathbf{a}_n, \mathbf{a}_{-n}\right)$ can be equivalently expressed as

$$\begin{aligned}\Phi\left(\mathbf{a}_n, \mathbf{a}_{-n}\right) = C_n\left(\mathbf{a}_n, \mathbf{a}_{-n}\right) &+ \sum_{\mathrm{SBS}_j \in \mathcal{Z}_n} C_j\left(\mathbf{a}_n, \mathbf{a}_{-n}\right) \\ &+ \sum_{\mathrm{SBS}_q \in \mathcal{T}_n} C_q\left(\mathbf{a}_n, \mathbf{a}_{-n}\right).\end{aligned} \tag{17}$$

When SBS_n unilaterally deviates its action from $\mathbf{a}_n$ to $\mathbf{a}_n'$, the change in the potential function is given by

$$\begin{aligned}&\Phi\left(\mathbf{a}_n, \mathbf{a}_{-n}\right) - \Phi\left(\mathbf{a}_n', \mathbf{a}_{-n}\right) \\ &\quad= C_n\left(\mathbf{a}_n, \mathbf{a}_{-n}\right) - C_n\left(\mathbf{a}_n', \mathbf{a}_{-n}\right) \\ &\qquad+ \sum_{\mathrm{SBS}_j \in \mathcal{Z}_n}\left(C_j\left(\mathbf{a}_n, \mathbf{a}_{-n}\right) - C_j\left(\mathbf{a}_n', \mathbf{a}_{-n}\right)\right) \\ &\qquad+ \sum_{\mathrm{SBS}_q \in \mathcal{T}_n}\left(C_q\left(\mathbf{a}_n, \mathbf{a}_{-n}\right) - C_q\left(\mathbf{a}_n', \mathbf{a}_{-n}\right)\right).\end{aligned} \tag{18}$$

By definition, the action change of SBS_n will only affect the aggregate inter-cell and intra-cell interference of itself and the inter-cell interference of SBSs in $\mathcal{Z}_n$. So we have $I_{\text{inter}}^{(q,k)}\left(\mathbf{a}_n, \mathbf{a}_{-n}\right) = I_{\text{inter}}^{(q,k)}\left(\mathbf{a}_n', \mathbf{a}_{-n}\right)$ and $I_{\text{intra}}^{(q,k)}\left(\mathbf{a}_n, \mathbf{a}_{-n}\right) = I_{\text{intra}}^{(q,k)}\left(\mathbf{a}_n', \mathbf{a}_{-n}\right)$ for any SBS_q in $\mathcal{T}_n$. In consequence, for any SBS_q in $\mathcal{T}_n$, we have

$$\begin{aligned}&C_q\left(\mathbf{a}_n, \mathbf{a}_{-n}\right) - C_q\left(\mathbf{a}_n', \mathbf{a}_{-n}\right) \\ &= \sum_{k=1}^{K_q}\left(B\log_2\left(1+\frac{p_{q,k}d_{q,q,k}^{-\alpha}}{I_{\text{inter}}^{(q,k)}\left(\mathbf{a}_n, \mathbf{a}_{-n}\right)+I_{\text{intra}}^{(q,k)}\left(\mathbf{a}_n, \mathbf{a}_{-n}\right)+\sigma^2}\right)\right. \\ &\quad\left.-B\log_2\left(1+\frac{p_{q,k}d_{q,q,k}^{-\alpha}}{I_{\text{inter}}^{(q,k)}\left(\mathbf{a}_n', \mathbf{a}_{-n}\right)+I_{\text{intra}}^{(q,k)}\left(\mathbf{a}_n', \mathbf{a}_{-n}\right)+\sigma^2}\right)\right) \\ &= 0.\end{aligned} \tag{19}$$

So (18) can be rewritten as

$$\begin{aligned}&\Phi\left(\mathbf{a}_n, \mathbf{a}_{-n}\right) - \Phi\left(\mathbf{a}_n', \mathbf{a}_{-n}\right) \\ &\quad= C_n\left(\mathbf{a}_n, \mathbf{a}_{-n}\right) - C_n\left(\mathbf{a}_n', \mathbf{a}_{-n}\right) \\ &\qquad+ \sum_{\mathrm{SBS}_j \in \mathcal{Z}_n}\left(C_j\left(\mathbf{a}_n, \mathbf{a}_{-n}\right) - C_j\left(\mathbf{a}_n', \mathbf{a}_{-n}\right)\right).\end{aligned} \tag{20}$$

Comparing (20) with the utility definition in (13) for SBS_n, we can reach the desired result that

$$\Phi\left(\mathbf{a}_n, \mathbf{a}_{-n}\right) - \Phi\left(\mathbf{a}_n', \mathbf{a}_{-n}\right) = u_n\left(\mathbf{a}_n, \mathbf{a}_{-n}\right) - u_n\left(\mathbf{a}_n', \mathbf{a}_{-n}\right), \tag{21}$$

which satisfies the definition of exact potential game [35] with Φ serving as the potential function. Due to the property of exact potential game, at least one NE is guaranteed. Moreover, noting that the potential function in (16) is exactly the same as the network utility in (10), we can conclude that solution $\mathbf{A}_{\text{opt}}$ for network utility maximization also globally maximizes the potential function, and hence is a NE of the game [35]. ■

IV. DISTRIBUTED LEARNING ALGORITHM

In this section, we design distributed learning algorithms to find the pure strategy NE of the formulated game. For exact potential games, best response (BR) and spatial adaptive play (SAP) algorithms are two efficient distributed learning algorithms that can achieve the pure strategy NE. However, for standard BR and SAP algorithms, only one player is allowed to update its action in each iteration, which severely influence the efficiency of the algorithm, especially when the SBSs are densely deployed. Noting that SBSs are coupled only locally but not globally according to G_{IM}, we extend the standard BR and SAP algorithms to their concurrent versions, i.e., concurrent BR (C-BR) and concurrent SAP (C-SAP), which admit rapid convergence to the pure strategy NE.

A. CONCURRENT BEST RESPONSE ALGORITHM

1) DESCRIPTION OF C-BR ALGORIGHM

The key idea of C-BR algorithm is that, in one iteration, a SBS proposes to change its strategy if a new strategy can bring in better utility based on the information it received. There may be several SBSs that have strategy update proposal, hence all these candidate SBSs contends for the update chance. The active SBSs are randomly picked, and when a SBS, e.g., SBS_n, is selected, other candidate SBSs which are also in $\mathcal{J}_n \cup \mathcal{Z}_n$ should be silenced in this iteration. Note that in standard BR algorithm, when SBS_n is selected, all other candidate SBSs are silenced whether they are in $\mathcal{J}_n \cup \mathcal{Z}_n$ or not. The selection procedure will continue until all candidate SBSs are either selected or silenced. The iteration loop stops when no SBS proposes to update its strategy or the maximum iteration step $T_{\max}$ is reached. The detail of the C-BR algorithm is given in Algorithm 1.

Algorithm 1 The C-BR Algorithm

Initialization: Each $\text{SBS}_n \in \mathcal{N}$ classifies its neighboring SBSs into $\mathcal{J}_n$ and $\mathcal{Z}_n$, and randomly selects a strategy $\mathbf{a}_n(0) \in \mathcal{A}_n$, where $\mathbf{a}_n(t)$ is the selected strategy of SBS_n at the t-th iteration.
for $t = 1$ **to** $T_{\max}$ **do**
  Search for best strategy: Each SBS_n gathers the experienced aggregate interference $I_{\text{inter}}^{(n,k)}$ and $I_{\text{intra}}^{(n,k)}$, and the signal power $p_{n,k}d_{n,n,k}^{-\alpha}$ from each of its associated UEs.
  Each SBS_n broadcasts its current strategy to SBSs in $\mathcal{J}_n \cup \mathcal{Z}_n$, and its signal power and aggregate interference to SBSs in $\mathcal{J}_n$.
  Based on its received information, each SBS_n calculates its best strategy $\mathbf{a}_n^*(t)$ as

$$\mathbf{a}_n^*(t) = \arg\max_{\mathbf{a}_n \in \mathcal{A}_n} u_n\left(\mathbf{a}_n, \mathbf{a}_{\mathcal{J}_n}(t), \mathbf{a}_{\mathcal{Z}_n}(t)\right). \tag{22}$$

  Contend to update strategy: Construct set $\mathcal{S}(t) = \left\{\text{SBS}_n | \text{SBS}_n \in \mathcal{N}, \mathbf{a}_n(t-1) \neq \mathbf{a}_n^*(t)\right\}$, and $\mathcal{U}(t) = \emptyset$.
  if $\mathcal{S}(t) \neq \emptyset$ **then**
    while $\mathcal{S}(t) \neq \emptyset$ **do**
      Randomly pick a SBS_n from $\mathcal{S}(t)$ and update its strategy, i.e., $\mathbf{a}_n(t) \leftarrow \mathbf{a}_n^*(t)$.
      $\mathcal{S}(t) \leftarrow \mathcal{S}(t) \backslash (\{\text{SBS}_n\} \cup \mathcal{Z}_n \cup \mathcal{J}_n)$.
      $\mathcal{U}(t) \leftarrow \mathcal{U}(t) \cup \{\text{SBS}_n\}$.
    end while
    Each SBS_n in $\mathcal{U}(t)$ keeps its strategy unchanged, i.e., $\mathbf{a}_n(t) \leftarrow \mathbf{a}_n(t-1)$.
  else
    Stop iteration.
  end if
end for

2) CONVERGENCE AND OPTIMALITY ANALYSIS FOR C-BR

Either the standard BR or the C-BR algorithm ensures an increasing trend for the potential function. Besides, the formulated locally cooperative game are with finite strategies. Therefore, according to [35], the formulated game has a finite improvement property (FIP), which implies that the BR-based algorithms are guaranteed to converge to the NE within a finite number of iterations. According to Theorem 1, the solution obtained by BR-based algorithms is locally or globally optimal.

B. CONCURRENT SPATIAL ADAPTIVE PLAY ALGORITHM

1) DESCRIPTION OF C-SAP ALGORITHM

Although BR-based algorithms rapidly converge to the NE of the game, these algorithms have evident drawback that the obtained NE may be locally optimal. To overcome this drawback, we also propose the SAP-based algorithms, which are featured with the capability of achieving the globally optimal pure strategy NE with an arbitrary large probability. The main technical difference between the SAP and the BR algorithms lies in the strategy updating rule for each SBS during the iteration. For the BR algorithm, the best strategy is deterministically selected for a SBS in each iteration, whereas, for the SAP algorithm, the subchannel assignment is determined in a stochastic manner. In specific, for the SAP algorithm, denote by $q_{n,s}(t)$ the probability that SBS_n selects its s-th subchannel assignment strategy in $\mathcal{A}_n$ at the t-th iteration. The selection probabilities for all strategies in $\mathcal{A}_n$ constitute the mixed strategy vector denoted by $\mathbf{q}_n(t)$ for SBS_n. The mixed strategy will be iteratively updated according to (23) given as

$$q_{n,s}(t) = \frac{\exp\left(\mu(t)u_n\left(\mathbf{a}_{n,s}, \mathbf{a}_{-n}\right)\right)}{\sum_{s'=1}^{|\mathcal{A}_n|}\exp\left(\mu(t)u_n\left(\mathbf{a}_{n,s'}, \mathbf{a}_{-n}\right)\right)}, \tag{23}$$

where $\mu(t)$ is the positive learning parameter monotonically increasing with t, and $\mathbf{a}_{n,s}$ is the s-th strategy in $\mathcal{A}_n$. When updating its mixed strategy, SBS_n assumes that all other SBSs will keep their strategies unchanged as $\mathbf{a}_{-n}$ and calculates for each strategy the expected utility, i.e., $u_n\left(\mathbf{a}_{n,s}, \mathbf{a}_{-n}\right)$ for $s \in \{1, \cdots, |\mathcal{A}_n|\}$. It is revealed in (23) that when $t \to \infty$, we will have $\mu(t) \to \infty$ and one of the selection probabilities will approach one, implying that the mixed strategy will converge to the pure strategy. In addition, similar to the BR algorithm, the SAP algorithm admits a concurrent version, which is termed the C-SAP algorithm and converges more rapidly than the standard version. The detail of the C-SAP algorithm is given in Algorithm 2.

Algorithm 2 The C-SAP Algorithm

Initialization: Each $\mathrm{SBS}_n \in \mathcal{N}$ classifies its neighboring SBSs into $\mathcal{J}_n$ and $\mathcal{Z}_n$, sets mixed strategy $q_{n,s}(0) = \frac{1}{|\mathcal{A}_n|}$, $\forall s \in \{1, \cdots, |\mathcal{A}_n|\}$, and randomly selects a strategy $\mathbf{a}_n(0) \in \mathcal{A}_n$ according to $\mathbf{q}_n(0)$, where $\mathbf{a}_n(t)$ is the selected strategy of SBS_n at the t-th iteration.

for $t = 1$ **to** $T_{\max}$ **do**

  Update mixed strategy vector: Each SBS_n gathers the experienced aggregate interference $I_{\text{inter}}^{(n,k)}$ and $I_{\text{intra}}^{(n,k)}$, and the signal power $p_{n,k}d_{n,n,k}^{-\alpha}$ from each of its associated UEs.

  Each SBS_n broadcasts its current strategy to SBSs in $\mathcal{J}_n \cup \mathcal{Z}_n$, and its signal power and aggregate interference to SBSs in $\mathcal{J}_n$.

  Based on its received information, each SBS_n updates its mixed strategy vector $\mathbf{q}_n(t)$ by

$$q_{n,s}(t) = \frac{\exp\left(\mu(t)u_n\left(\mathbf{a}_{n,s}, \mathbf{a}_{-n}\right)\right)}{\sum_{s'=1}^{|\mathcal{A}_n|}\exp\left(\mu(t)u_n\left(\mathbf{a}_{n,s'}, \mathbf{a}_{-n}\right)\right)}, \tag{24}$$

  Each SBS_n randomly selects its strategy $\mathbf{a}_n^*(t)$ according to $\mathbf{q}_n(t)$.

  Contend to update strategy: Construct set $\mathcal{S}(t) = \left\{\mathrm{SBS}_n | \mathrm{SBS}_n \in \mathcal{N}, \mathbf{a}_n(t-1) \neq \mathbf{a}_n^*(t)\right\}$, and $\mathcal{U}(t) = \emptyset$.

  if $\mathcal{S}(t) \neq \emptyset$ **then**

    while $\mathcal{S}(t) \neq \emptyset$ **do**

      Randomly pick a SBS_n from $\mathcal{S}(t)$ and update its strategy, i.e., $\mathbf{a}_n(t) \leftarrow \mathbf{a}_n^*(t)$.

      $\mathcal{S}(t) \leftarrow \mathcal{S}(t) \backslash \left(\{\mathrm{SBS}_n\} \cup \mathcal{Z}_n \cup \mathcal{J}_n\right)$.

      $\mathcal{U}(t) \leftarrow \mathcal{U}(t) \cup \{\mathrm{SBS}_n\}$.

    end while

    Each SBS_n in $\mathcal{U}(t)$ keeps its strategy unchanged, i.e., $\mathbf{a}_n(t) \leftarrow \mathbf{a}_n(t-1)$.

  else

    Stop iteration.

  end if

end for

2) CONVERGENCE AND OPTIMALITY ANALYSIS FOR C-SAP

We now characterize the convergence and optimality property for the C-SAP algorithm. We firstly prove that, with the C-SAP algorithm, a unique stationary distribution exists for different subchannel assignment profiles. Then we prove that the converged profile under the C-SAP algorithm will be the optimal one with an arbitrary large probability.

Theorem 2: With the C-SAP algorithm, a unique stationary distribution π_i exists for subchannel assignment profile $\mathbf{A}_i \in \mathcal{A}$ when $\mu > 0$, and is given as

$$\pi_i = \frac{\exp\left(\mu\Phi(\mathbf{A}_i)\right)}{\sum_{\mathbf{A}_t\in\mathcal{A}}\exp\left(\mu\Phi\left(\mathbf{A}_t\right)\right)}, \tag{25}$$

where $\Phi(\mathbf{A})$ is the potential function defined in (16) given the subchannel assignment profile being $\mathbf{A}$, and $\mathcal{A}$ is the set constituted by all possible subchannel assignment profiles.

Proof: Let $\mathbf{A}_j \in \mathcal{A}$ be another arbitrary selected subchannel assignment profile which is different from $\mathbf{A}_i$. Assume that, compared with $\mathbf{A}_i$, totally V SBSs are with different subchannel assignments in $\mathbf{A}_j$. So the SBS set can be split as $\mathcal{N} = \left\{\mathrm{SBS}_{n_1}, \cdots, \mathrm{SBS}_{n_v}, \cdots, \mathrm{SBS}_{n_V}\right\} \cup \left\{\mathrm{SBS}_{n_{V+1}}, \mathrm{SBS}_{n_{V+2}}, \cdots, \mathrm{SBS}_{n_N}\right\}$, in which the former subset is constituted by the SBSs with different subchannel assignments in $\mathbf{A}_i$ and $\mathbf{A}_j$. Let $s_{n,i} \in \{1, \cdots, |\mathcal{A}_n|\}$ and $s_{n,j} \in \{1, \cdots, |\mathcal{A}_n|\}$ index the strategies of SBS_n designated by $\mathbf{A}_i$ and $\mathbf{A}_j$. Therefore we have $s_{n,i} \neq s_{n,j}$ for $n \in \mathcal{V} = \{n_1, \cdots, n_v, \cdots, n_V\}$ and $s_{n,i} = s_{n,j}$ for $n \in \{n_{V+1}, n_{V+2}, \cdots, n_N\}$. Due to the fact that $\mathbf{A}$ is obviously a discrete time Markov process, which is irreducible and aperiodic, there exists an unique stationary distribution for $\mathbf{A}$. Note that $\mathbf{A}_i$ and $\mathbf{A}_j$ are also referred to as two states of the system.

Then we verify that the distribution in (25) satisfies the detailed balance equation (DBE) of the Markov process, which suffices to prove that (25) is the unique stationary distribution. Denote by $\mathscr{P}_{i\to j}$ the state transition probability from $\mathbf{A}_i$ to $\mathbf{A}_j$. To transit from $\mathbf{A}_i$ to $\mathbf{A}_j$, each $\mathrm{SBS}_n \in \left\{\mathrm{SBS}_{n_1}, \cdots, \mathrm{SBS}_{n_V}\right\}$ should change its strategy from $\mathbf{a}_{n,s_{n,i}}$ to $\mathbf{a}_{n,s_{n,j}}$, and the transition probability is calculated according to (23) as

$$q_{n,s_{n,j}} = \frac{\exp\left(\mu u_n\left(\mathbf{a}_{n,s_{n,j}}\right)\right)}{\sum_{s=1}^{|\mathcal{A}_n|}\exp\left(\mu u_n\left(\mathbf{a}_{n,s}\right)\right)}. \tag{26}$$

In each iteration, the mixed strategies of different SBSs are updated independently, so $\mathscr{P}_{i\to j}$ can be rewritten as

$$\mathscr{P}_{i\to j} = \prod_{n\in\mathcal{V}} q_{n,s_{n,j}} = \prod_{n\in\mathcal{V}} \frac{\exp\left(\mu u_n\left(\mathbf{a}_{n,s_{n,j}}\right)\right)}{\sum_{s=1}^{|\mathcal{A}_n|}\exp\left(\mu u_n\left(\mathbf{a}_{n,s}\right)\right)}. \tag{27}$$

So we have

$$\begin{aligned}
&\pi_i\mathscr{P}_{i\to j} \\
&= \frac{\exp\left(\mu\Phi(\mathbf{A}_i)\right)}{\sum_{\mathbf{A}_t\in\mathcal{A}}\exp\left(\mu\Phi\left(\mathbf{A}_t\right)\right)} \prod_{n\in\mathcal{V}} \frac{\exp\left(\mu u_n\left(\mathbf{a}_{n,s_{n,j}}\right)\right)}{\sum_{s=1}^{|\mathcal{A}_n|}\exp\left(\mu u_n\left(\mathbf{a}_{n,s}\right)\right)} \\
&= \underbrace{\frac{1}{\sum_{\mathbf{A}_t\in\mathcal{A}}\exp\left(\mu\Phi\left(\mathbf{A}_t\right)\right)} \prod_{n\in\mathcal{V}} \frac{1}{\sum_{s=1}^{|\mathcal{A}_n|}\exp\left(\mu u_n\left(\mathbf{a}_{n,s}\right)\right)}}_{\lambda} \\
&\quad \times \exp\left(\mu\left(\Phi\left(\mathbf{A}_i\right) + \prod_{n\in\mathcal{V}} u_n\left(\mathbf{a}_{n,s_{n,j}}\right)\right)\right).
\end{aligned} \tag{28}$$

According to Theorem 1, the formulated game is an exact potential game, which implies that

$$\Phi\left(\mathbf{A}_i\right) - \Phi\left(\mathbf{A}_j\right) = \prod_{n\in\mathcal{V}}\left(u_n\left(\mathbf{a}_{n,s_{n,i}}\right) - u_n\left(\mathbf{a}_{n,s_{n,j}}\right)\right). \tag{29}$$

Therefore (28) can be rewritten as

$$\begin{aligned}
&\pi_i \mathscr{P}_{i\to j} \\
&= \lambda \exp\left(\mu\left(\Phi\left(\mathbf{A}_i\right) + \prod_{n\in\mathcal{V}} u_n\left(\mathbf{a}_{n,s_{n,j}}\right)\right)\right) \\
&= \lambda \exp\left(\mu\left(\Phi\left(\mathbf{A}_j\right) + \prod_{n\in\mathcal{V}} u_n\left(\mathbf{a}_{n,s_{n,i}}\right)\right)\right) \\
&= \underbrace{\frac{\exp\left(\mu\Phi(\mathbf{A}_j)\right)}{\sum_{\mathbf{A}_t\in\mathcal{A}}\exp\left(\mu\Phi\left(\mathbf{A}_t\right)\right)}}_{\pi_j} \underbrace{\prod_{n\in\mathcal{V}} \frac{\exp\left(\mu u_n\left(\mathbf{a}_{n,s_{n,i}}\right)\right)}{\sum_{s=1}^{|\mathcal{A}_n|}\exp\left(\mu u_n\left(\mathbf{a}_{n,s}\right)\right)}}_{\mathscr{P}_{j\to i}} \\
&= \pi_j \mathscr{P}_{j\to i}, \qquad (30)
\end{aligned}$$

which satisfies the DBE of the Markov process. This completes the proof. ■

Theorem 2 provides the stationary probability of the converged subchannel assignment profile. Now we discuss the optimality of the C-SAP algorithm in Theorem 3.

Theorem 3: Given a sufficiently large learning parameter μ, the C-SAP algorithm converges to the globally optimal solution $\mathbf{A}_{\text{opt}}$ with an arbitrarily large probability.

Proof: According to (11) and (16), we have $\Phi\left(\mathbf{A}_{\text{opt}}\right) = \max U(\mathbf{A}) > 0$. Hence, when $\mu \to \infty$, we have

$$\exp\left(\mu\Phi\left(\mathbf{A}_{\text{opt}}\right)\right) \gg \exp\left(\mu\Phi\left(\mathbf{A}_t\right)\right), \quad \forall \mathbf{A}_t \in \mathcal{A}\backslash\mathbf{A}_{\text{opt}}. \qquad (31)$$

The stationary distribution of π_{opt} can be rewritten as

$$\begin{aligned}
&\lim_{\mu\to\infty} \pi_{\text{opt}} \\
&= \frac{\exp\left(\mu\Phi\left(\mathbf{A}_{\text{opt}}\right)\right)}{\sum_{\mathbf{A}_t\in\mathcal{A}\backslash\mathbf{A}_{\text{opt}}}\exp\left(\mu\Phi\left(\mathbf{A}_t\right)\right) + \exp\left(\mu\Phi\left(\mathbf{A}_{\text{opt}}\right)\right)} = 1. \qquad (32)
\end{aligned}$$

This completes the proof. ■

It should be noted that the learning parameter μ plays an important role in the SAP-based algorithms since it appears in both the updating rule in (23) as well as the stationary distribution in (25). In specific, when a SBS selects its strategy according to (23), the difference in the probabilities of the alternative strategies will be narrow if μ is small. For example, setting $\mu = 0$ will make a SBS select any strategy under equal probabilities. On the contrary, if μ is set to be a large value, the strategies bringing in higher utilities in that iteration will be more likely to be selected. For example, setting $\mu \to \infty$ will make a SBS deterministically select the best strategy in that iteration, which is the same as the BR-based algorithms. In a word, a small value of μ will be more efficient for the SAP-based algorithms to escape from a local optimum and search for a better NE, while a large value of μ will lead to the convergence and prevent the algorithm from fluctuating among different good solutions. Therefore, it is recommended that, the learning parameter be set as a small value at the beginning of the iteration to explore better possible NEs and gradually increases with the iteration index to exploit the optimal current strategy and converge. Upon this guidance, we set the learning parameter as $\mu(t) = \beta \cdot t$ in the simulation, where β is the learning step balancing the tradeoff between exploration and exploitation, and t is the iteration index.

V. SIMULATION RESULTS AND DISCUSSION

In this section, we provide MATLAB based simulation results to evaluate the proposed distributed algorithms. The SBSs are randomly deployed in a square region to form a SCN. The number of associated UEs for each SBS is assumed to be identical as $K_n = K$. The serving area for each SBS is assumed to be a circle with a radius of 10 m. Each SBS transmits with equal power $p_n = 2$ W on each of its occupied subchannels. The path-loss exponent is fixed as $\alpha = 3.7$, the NOMA power proportional decay factor is $\eta = 0.4$, and the IM threshold is $I_{\text{th}} = 0.001$. Totally $M = 5$ subchannels are available in the system, and the bandwidth of each subchannel is 100 kHz. The power of the noise is set to be -174 dBm/Hz.

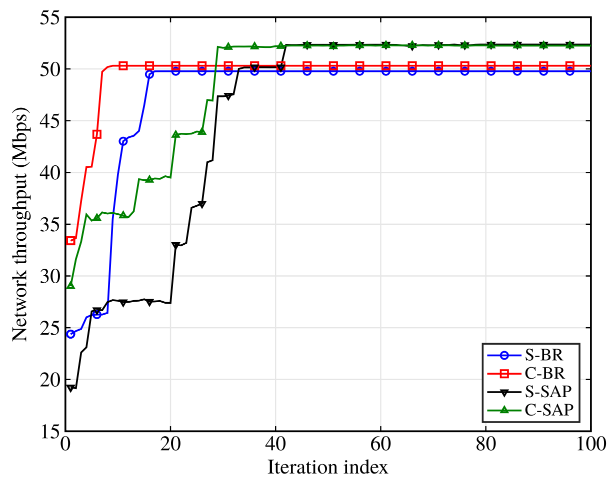

FIGURE 3. Converging procedure of the S-BR, S-SAP, C-BR, and C-SAP algorithms, with 10 SBSs randomly deployed in a 100 × 100 m^2 area, $\beta = 0.001$, and $K = 3$.

In Fig. 3, the convergence procedure of the S-BR, C-BR, S-SAP, and C-SAP algorithms are illustrated. It is revealed that, the proposed algorithms all converge after a number of iterations. For the BR-based algorithms, the iterations converge at a much faster speed than the SAP-based algorithms, but the converged throughput performance is poorer. This is due to the difference in the updating rules that the BR-based algorithms deterministically select the best strategy for each SBS in each iteration, which guarantees a faster convergence speed but may easily get trapped at the local optimal solution. Whereas, the SAP-based algorithms update strategies in a stochastic manner, which brings in the superiority of escaping from the local optimum as well as the deficiency of a slower converging speed. This stochastic manner also explains the observation that the curves for the SAP algorithms may fluctuate at some iterations in spite of the overall converging trend. Meanwhile, we also compare the standard and concurrent algorithms from the aspects of the converging speed and the network throughput for both the BR-based and SAP-based algorithms. For the SAP-based algorithms, we can see that the C-SAP algorithm requires fewer iterations than the S-SAP algorithm to converge. This shows the advantage of the C-SAP algorithm over the S-SAP algorithm in the aspect of converging speed, which is brought in by allowing multiple uncoupled SBSs to update their strategies simultaneously. Besides, the converged performance of the C-SAP and S-SAP algorithms are almost the same. This is because, in the C-SAP algorithm, the SBSs that are allowed to update strategies in the same iteration are uncoupled in G_{IM}. Simultaneously updating the strategies of multiple uncoupled SBSs will not influence the optimality efficiency of the converged solution. Similar results can be observed by comparing the C-BR and S-BR algorithms.

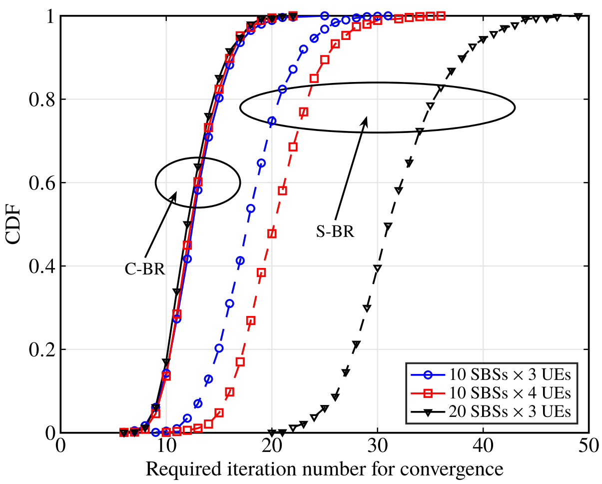

FIGURE 4. Converging speed comparison between C-BR and S-BR algorithms under different network size.

Fig. 4 presents the cumulative distribution function (CDF) of the required convergence iteration number for the BR-based algorithms to further illustrate the advantages of the concurrent algorithms over the standard algorithms. Simulation results are obtained under the same SBS density in different area assumptions, i.e., 100×100 m^2 for $N = 10$ and $100\sqrt{2} \times 100\sqrt{2}$ m^2 for $N = 20$. The advantage of the concurrent algorithms in the aspect of converging speed is confirmed as discussed in the results of Fig. 3. Another observation is that, the superiority of the concurrent algorithm is more evident when the network size is scaled up. In specific, the standard algorithm will require much more iterations to converge whether the simulation area size is extended or more served UEs are added for a SBS. But for the concurrent algorithm, the required number of iterations only slightly varies.

In Fig. 5, the converged average SBS throughput performance of the C-BR and C-SAP algorithms are compared with that of the random selection and exhaust search solutions. The results of the C-BR and C-SAP algorithms are

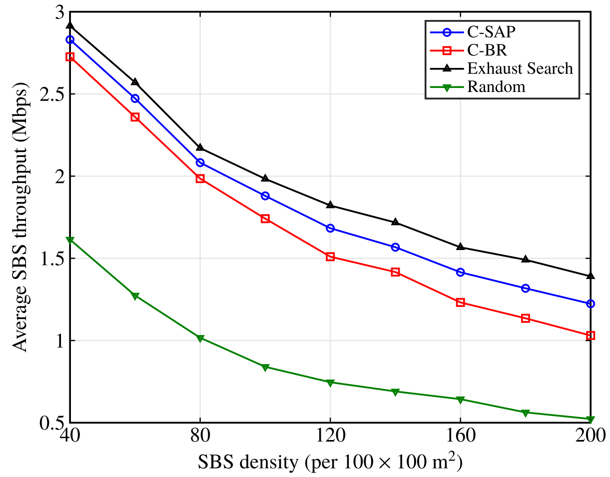

FIGURE 5. Average SBS throughput v.s. SBS density under different algorithms, with fixed 20 SBSs but linearly scaled area, $K = 3$, and $\beta = 0.0001$.

averaged over 5 independent random network topologies through 5000 trials. Note that the exhaustive search is extremely time consuming since the number of the possible subchannel assignment profile is quite large, i.e., $5^{3\times 20} \approx 8.6 \times 10^{41}$. So we alternatively use the best results obtained through C-BR algorithm to approximate the exhaustive search results. It is revealed that the average SBS throughput performance monotonically degrades with the SBS density for all algorithms, which is due to the increased interference level. We can also see that the converged throughput performance of the C-SAP algorithm is better than the C-BR algorithm with a much smaller gap to the results obtained by the exhaustive search solution. This advantage is due to the stochastic selection feature of the C-SAP algorithm, which helps the iteration escape from the local optimum. In addition, both the C-BR and C-SAP algorithms significantly outperform the random selection.

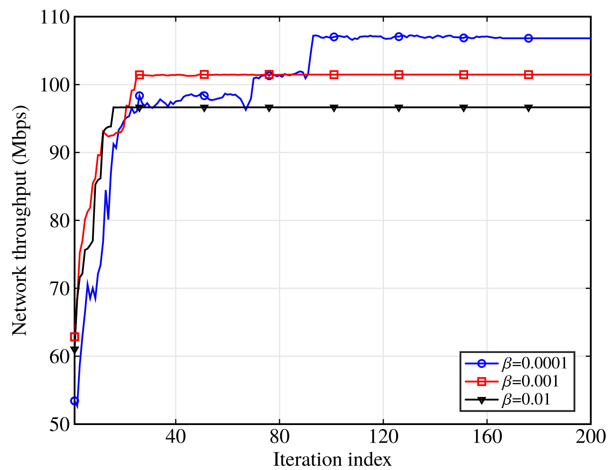

FIGURE 6. Converging speed comparison for the C-SAP algorithm under different learning steps, with 20 SBSs randomly deployed in a $100\sqrt{2} \times 100\sqrt{2}$ m^2 area, and $K = 3$.

In Fig. 6 and 7, we investigate the impact of the learning parameter on the converging speed and the converged

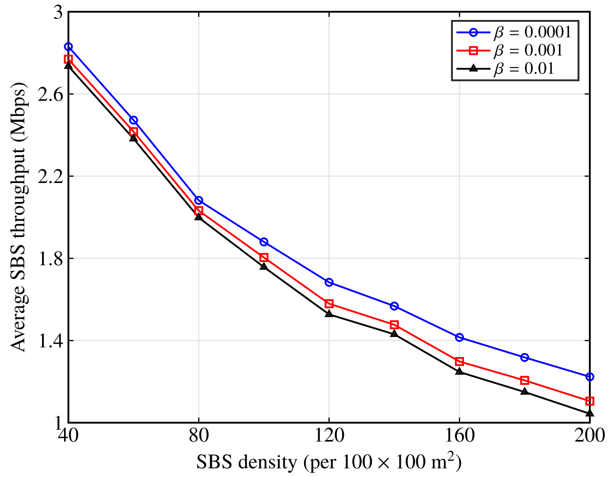

FIGURE 7. Average SBS throughput v.s. SBS density under different learning steps, with fixed 20 SBSs but linearly scaled area, and $K = 3$.

throughput performance of the C-SAP algorithm. Fig. 6 shows that a larger learning step β will lead to a faster converging speed for the C-SAP algorithm. When $\mu(t) = 0.01t$, the algorithm requires fewer than 20 iterations to converge, but when $\mu(t) = 0.0001t$, the converging procedure extends to more than 100 iterations. The reason is that decreasing the learning step β will require a larger iteration index t to make the selection probability of the optimal strategy approach one. Nontheless, a small learning step helps the algorithm explore better solutions during the iteration, with the network throughput curve for $\beta = 0.0001$ being the highest one. Fig. 7 reveals similar results as Fig. 6 that the C-SAP algorithm will converge with a better throughput performance if the learning step is set to be a smaller value.

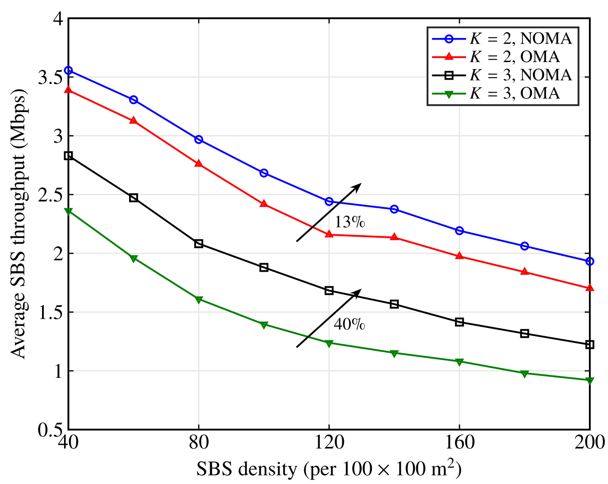

FIGURE 8. Throughput performance comparison between NOMA and OMA under the C-SAP algorithm and different serving UE numbers, with fixed 20 SBSs but linearly scaled area, and $\beta = 0.0001$.

In Fig. 8, we plot the converged average SBS throughput obtained through the C-SAP algorithm to investigate the advantage of NOMA over OMA. It is shown that NOMA obviously brings in a higher average throughput than traditional OMA. To explain this advantage, recall that the NOMA technique provides an opportunity for the network to profit as follows: 1) When only one of the several subchannels is lightly interfered, a SBS can apply NOMA to serve multiple UEs on this subchannel and let them share the benefit of the low inter-cell interference if the intra-cell interference is not severe, which meets with the selfish nature of an individual SBS. 2) When a SBS applies NOMA, it can release its occupancy of some other subchannels and thus reduce its interference to the nearby SBSs occupying the same subchannels, which altruistically makes profit for the whole network although the throughput of this SBS may be influenced. Fig. 8 also shows a relatively larger performance gap between NOMA and OMA with the increase in the serving UE number, i.e., the throughput approximately increases 13% for $K = 2$, and 40% for $K = 3$. This implies that the superiority of NOMA is more evident when the network is heavily loaded.

VI. CONCLUSION

In this paper, we explored the potential of NOMA in interference mitigation for the downlink SCN. By opportunistically applying NOMA, we proactively introduced intra-cell interference to balance the severe inter-cell interference brought in by ultra dense networking, which was different from previous work in the NOMA literature. We considered subchannel assignment problem to maximize the network throughput. To this end, we formulated a locally cooperative game to motivate SBSs to act in a locally altruistic manner, as well as to study the interaction between SBSs. The existence of NE was validated in the formulated game by proving it as an exact potential game, and two concurrent distributed learning algorithms were proposed to converge towards the NE with boosted converging speed. Simulation results showed that: 1) The proposed two concurrent distributed algorithms both converge to the NE of the game, and the converging speed is faster than their standard versions. 2) The SAP-based algorithm provides a learning parameter to balance the converging speed and the efficiency of the optimum, whereas the BR-based algorithm converges with the fastest speed but the converged solution is very likely to be trapped in the local optimum. 3) Compared with OMA, NOMA further enhances the performance of distributed interference mitigation in SCN, and this leads to higher network throughput for the system.

The work in this paper allows several extensions in the future work. The first is applying advanced learning algorithms, e.g., stochastic learning automata, to further reduce the amount of information exchange between SBSs. The second direction can be jointly taking into account the feature of WiFi and NOMA to design new protocols for balancing the interference between the WiFi networks and the LTE-unlicensed band communications. Besides, noting that the realistic user throughput demands are different and that NOMA has a great potential in increasing the overall quality of experience (QoE), our work can also be extended from the user-centric perspective.

REFERENCES

[1] A. Osseiran *et al.*, "Scenarios for 5G mobile and wireless communications: The vision of the METIS project," *IEEE Commun. Mag.*, vol. 52, no. 5, pp. 26–35, May 2014.

[2] J. G. Andrews *et al.*, "What will 5G be?" *IEEE J. Sel. Areas Commun.*, vol. 32, no. 6, pp. 1065–1082, Jun. 2014.

[3] X. Ge, S. Tu, G. Mao, C.-X. Wang, and T. Han, "5G ultra-dense cellular networks," *IEEE Wireless Commun. Mag.*, vol. 23, no. 1, pp. 29–72, Feb. 2016.

[4] H. Zhang, S. Huang, C. Jiang, K. Long, V. C. M. Leung, and H. V. Poor, "Energy efficient user association and power allocation in millimeter-wave-based ultra dense networks with energy harvesting base stations," *IEEE J. Sel. Areas Commun.*, vol. 35, no. 9, pp. 1936–1947, Sep. 2017.

[5] K. N. R. S. V. Prasad, E. Hossain, and V. K. Bhargava, "Energy efficiency in massive MIMO-based 5G networks: Opportunities and challenges," *IEEE Wireless Commun.*, vol. 24, no. 3, pp. 86–94, Jun. 2017.

[6] Z. Ding *et al.*, "Application of non-orthogonal multiple access in LTE and 5G networks," *IEEE Commun. Mag.*, vol. 55, no. 2, pp. 185–191, Feb. 2017.

[7] Z. Ding, X. Lei, G. K. Karagiannidis, R. Schober, J. Yuan, and V. Bhargava, "A survey on non-orthogonal multiple access for 5G networks: Research challenges and future trends," *IEEE J. Sel. Areas Commun.*, vol. 35, no. 10, pp. 2181–2195, Oct. 2017.

[8] Y. Liu, Z. Qin, M. Elkashlan, Z. Ding, A. Nallanathan, and L. Hanzo, "Nonorthogonal multiple access for 5G and beyond," *Proc. IEEE*, vol. 105, no. 12, pp. 2347–2381, Dec. 2017.

[9] Y. Saito, Y. Kishiyama, A. Benjebbour, T. Nakamura, A. Li, and K. Higuchi, "Non-orthogonal multiple access (NOMA) for cellular future radio access," in *Proc. IEEE Veh. Technol. Conf. (VTC Spring)*, Dresden, Germany, Jun. 2013, pp. 1–5.

[10] Z. Ding, L. Dai, and H. V. Poor, "MIMO-NOMA design for small packet transmission in the Internet of Things," *IEEE Access*, vol. 4, pp. 1393–1405, 2016.

[11] L. Lv, J. Chen, Q. Ni, and Z. Ding, "Design of cooperative non-orthogonal multicast cognitive multiple access for 5G systems: User scheduling and performance analysis," *IEEE Trans. Commun.*, vol. 65, no. 6, pp. 5825–5837, Jun. 2016.

[12] Z. Zhang, Z. Ma, M. Xiao, G. Liu, and P. Fan, "Modeling and analysis of non-orthogonal MBMS transmission in heterogeneous networks," *IEEE J. Sel. Areas Commun.*, vol. 35, no. 10, pp. 2221–2237, Oct. 2017.

[13] Y. Liu, X. Li, F. R. Yu, H. Ji, H. Zhang, and V. C. M. Leung, "Grouping and cooperating among access points in user-centric ultra-dense networks with non-orthogonal multiple access," *IEEE J. Sel. Areas Commun.*, vol. 35, no. 10, pp. 2295–2311, Oct. 2017.

[14] H. Tabassum, E. Hossain, and M. J. Hossain, "Modeling and analysis of uplink non-orthogonal multiple access in large-scale cellular networks using Poisson cluster process," *IEEE Trans. Commun.*, vol. 65, no. 8, pp. 3555–3570, Aug. 2017.

[15] M. Jia, D. Li, Z. Yin, Q. Guo, and X. Gu, "High spectral efficiency secure communications with non-orthogonal physical and multiple access layers," *IEEE Internet Things J.*, to be published.

[16] Y. Tian *et al.*, "On the performance of opportunistic NOMA in downlink CoMP networks," *IEEE Commun. Lett.*, vol. 20, no. 5, pp. 998–1001, May 2016.

[17] B. Di, L. Song, and Y. Li, "Sub-channel assignment, power allocation, and user scheduling for non-orthogonal multiple access networks," *IEEE Trans. Wireless Commun.*, vol. 15, no. 11, pp. 7686–7698, Nov. 2016.

[18] J. Zhao, Y. Liu, K. K. Chai, A. Nallanathan, Y. Chen, and Z. Han, "Spectrum allocation and power control for non-orthogonal multiple access in HetNets," *IEEE Trans. Wireless Commun.*, vol. 16, no. 9, pp. 5825–5837, Sep. 2017.

[19] F. Fang, H. Zhang, J. Cheng, and V. C. M. Leung, "Energy-efficient resource allocation for downlink non-orthogonal multiple access network," *IEEE Trans. Commun.*, vol. 64, no. 9, pp. 3722–3732, Sep. 2016.

[20] H. Zhang, B. Wang, C. Jiang, K. Long, A. Nallanathan, and V. C. M. Leung, "Energy efficient dynamic resource allocation in NOMA networks," in *Proc. IEEE Global Commun. Conf. (GLOBECOM)*, Singapore, Dec. 2017, pp. 1–6.

[21] L. P. Qian, Y. Wu, H. Zhou, and X. Shen, "Joint uplink base station association and power control for small-cell networks with non-orthogonal multiple access," *IEEE Trans. Wireless Commun.*, vol. 16, no. 9, pp. 5567–5582, Sep. 2017.

[22] W. Bao, H. Chen, Y. Li, and B. Vucetic, "Joint rate control and power allocation for non-orthogonal multiple access systems," *IEEE J. Sel. Areas Commun.*, vol. 35, no. 12, pp. 2798–2811, Dec. 2017.

[23] J. Liu, M. Sheng, L. Liu, and J. Li, "Interference management in ultra-dense networks: Challenges and approaches," *IEEE Netw.*, vol. 31, no. 6, pp. 70–77, Nov./Dec. 2017.

[24] Q. Wu *et al.*, "Cognitive Internet of Things: A new paradigm beyond connection," *IEEE Internet Things J.*, vol. 1, no. 2, pp. 129–143, Apr. 2014.

[25] M. Jia, Z. Yin, Q. Guo, G. Liu, and X. Gu, "Downlink design for spectrum efficient IoT network," *IEEE Internet Things J.*, to be published.

[26] Y. Xu, J. Wang, Q. Wu, Z. Du, L. Shen, and A. Anpalagan, "A game-theoretic perspective on self-organizing optimization for cognitive small cells," *IEEE Commun. Mag.*, vol. 53, no. 7, pp. 100–108, Jul. 2015.

[27] J. Zheng, Y. Cai, Y. Liu, Y. Xu, B. Duan, and X. Shen, "Optimal power allocation and user scheduling in multicell networks: Base station cooperation using a game-theoretic approach," *IEEE Trans. Wireless Commun.*, vol. 13, no. 12, pp. 6928–6942, Dec. 2014.

[28] Y. Xu *et al.*, "Load-aware dynamic spectrum access for small-cell networks: A graphical game approach," *IEEE Trans. Veh. Technol.*, vol. 65, no. 10, pp. 8794–8800, Oct. 2016.

[29] N. Zhang, S. Zhang, J. Zheng, X. Fang, J. W. Mark, and X. Shen, "QoE driven decentralized spectrum sharing in 5G networks: Potential game approach," *IEEE Trans. Veh. Technol.*, vol. 66, no. 9, pp. 7797–7808, Sep. 2017.

[30] Q. Wu, D. Wu, Y. Xu, and J. Wang, "Demand-aware multichannel opportunistic spectrum access: A local interaction game approach with reduced information exchange," *IEEE Trans. Veh. Technol.*, vol. 64, no. 10, pp. 4899–4904, Oct. 2015.

[31] X. Wang, H. Zhang, Y. Tian, Z. Ding, and V. C. M. Leung, "Locally cooperative interference mitigation for small cell networks with non-orthogonal multiple access: A potential game approach," in *Proc. IEEE Int. Conf. Commun. (ICC)*, Kansas City, MO, USA, May 2018, pp. 1–6.

[32] K. Yao, Q. Wu, Y. Xu, and J. Jing, "Distributed ABS-slot access in dense heterogeneous networks: A potential game approach with generalized interference model," *IEEE Access*, vol. 5, pp. 94–104, Feb. 2017.

[33] Y. Xu, J. Wang, Q. Wu, A. Anpalagan, and Y.-D. Yao, "Opportunistic spectrum access in cognitive radio networks: Global optimization using local interaction games," *IEEE J. Sel. Topics Signal Process.*, vol. 6, no. 2, pp. 180–194, Apr. 2012.

[34] Q. Wu, G. Ding, J. Wang, and Y. D. Yao, "Spatial-temporal opportunity detection for spectrum-heterogeneous cognitive radio networks: Two-dimensional sensing," *IEEE Trans. Wireless Commun.*, vol. 12, no. 2, pp. 516–526, Feb. 2013.

[35] D. Monderer and L. S. Shapley, "Potential games," *Games Econ. Behav.*, vol. 14, no. 1, pp. 124–143, 1996.

XIANLING WANG (M'15) received the B.S. degree in communication engineering and the Ph.D. degree in communication and information system from the School of Information and Communication Engineering, Beijing University of Posts and Telecommunications, China, in 2009 and 2014, respectively. He is currently an Assistant Professor with the Fujian Key Laboratory of Communication Network and Information Processing, Xiamen University of Technology, China. He has authored or co-authored several papers in international conferences and journals in his research area. His research interests include stochastic geometry, game theory, 5G wireless networks, UAV communication networks, and non-orthogonal multiple access.

HAIJUN ZHANG (M'13–SM'17) was a Post-Doctoral Research Fellow with the Department of Electrical and Computer Engineering, The University of British Columbia, Vancouver Campus, Canada. He is currently a Full Professor with the University of Science and Technology Beijing, China. He received the IEEE ComSoc Young Author Best Paper Award in 2017 and the IEEE CSIM Technical Committee Best Journal Paper Award in 2018. He has serves/served as a General Co-Chair for GameNets'16, a Symposium Chair for GLOBECOM'19, a TPC Co-Chair for the INFOCOM'18 Workshop IECCO, a General Co-Chair for the ICC'18/ICC'17/GLOBECOM'17 Workshop on UDN, and a General Co-Chair for the GLOBECOM'17 Workshop on LTE-U. He serves as an Editor for the IEEE Transactions on Communications, the IEEE Transactions on Green Communications and Networking, and the IEEE 5G Tech Focus, and has serves/served as a Leading Guest Editor for the *IEEE Communications Magazine* and the IEEE Transactions on Emerging Topics in Computing.

YUE TIAN (M'18) received the bachelor's degree from the Beijing University of Posts and Telecommunications in 2011 and the master's degree in wireless communication and signal processing and the Ph.D. degree in electrical engineering from the University of Bristol in 2012 and 2017, respectively. In 2017, he joined the School of Opto-Electronic and Communication Engineering, Xiamen University of Technology, as an Assistant Professor. His research focuses on 5G communication system techniques, such as interference alignment, massive MIMO, and non-orthogonal multiple access.

CHEN ZHU received the Ph.D. degree in communication and information system from Xiamen University in 2014. Her research focuses on key techniques of 5G communication system, including resource allocation, interference management, and cognitive radio. She is awarded several invent patents in related technical field.

VICTOR C. M. LEUNG (S'75–M'89–SM'97–F'03) received the B.A.Sc. degree (Hons.) in electrical engineering and the Ph.D. degree in electrical engineering, from The University of British Columbia (UBC) in 1977 and 1982, respectively. He received the APEBC Gold Medal as the Head of the 1977 Graduating Class with the UBC Faculty of Applied Science. He received a Canadian Natural Sciences and Engineering Research Council Postgraduate Scholarship in 1977–1981 to support his postgraduate studies. From 1981 to 1987, he was a Senior Member of Technical Staff and a Satellite System Specialist at MPR Teltech Ltd., Canada. In 1988, he was a Lecturer with the Department of Electronics, The Chinese University of Hong Kong. He returned to UBC as a Faculty Member in 1989, where he is currently a Professor and the TELUS Mobility Research Chair in Advanced Telecommunications Engineering with the Department of Electrical and Computer Engineering. He has co-authored over 1150 journal/conference papers and 40 book chapters. He has co-edited 14 book titles. His research interests are in the broad areas of wireless networks and mobile systems. Several of his papers had been selected for best paper awards.

Dr. Leung is a registered Professional Engineer in the Province of British Columbia, Canada. He was a Distinguished Lecturer of the IEEE Communications Society. He is a fellow of the Royal Society of Canada, the Engineering Institute of Canada, and the Canadian Academy of Engineering. He received the IEEE Vancouver Section Centennial Award, the 2011 UBC Killam Research Prize, the 2017 Canadian Award for Telecommunications Research, and the 2018 IEEE TGCC Distinguished Technical Achievement Recognition Award. He has co-authored papers that received the 2017 IEEE ComSoc Fred W. Ellersick Prize, the 2017 IEEE Systems Journal Best Paper Award, and the 2018 IEEE CSIM Best Journal Paper Award. He has served on the Editorial Boards for the IEEE Journal on Selected Areas in Communications-Wireless Communications Series and Series on Green Communications and Networking, the IEEE Transactions on Wireless Communications, the IEEE Transactions on Vehicular Technology, the IEEE Transactions on Computers, the IEEE Wireless Communications Letters, and the *Journal of Communications and Networks*. He is serving on the Editorial Boards for the IEEE Transactions on Green Communications and Networking, the IEEE Transactions on Cloud Computing, the IEEE Access, the IEEE Network, *Computer Communications*, and several other journals. He has guest-edited many journal special issues, and provided leadership to the organizing committees and technical program committees of numerous conferences and workshops.